

Stereoblock Polypropylene/Isotactic Polypropylene Blends.

I. Phase Organization

S. CANEVAROLO[†] and F. DE CANDIA^{*}

Dipartimento di Ingegneria Chimica e Alimentare, Università di Salerno, 84081 Fisciano (Salerno), Italy

SYNOPSIS

The phase organization of stereoblock polypropylene/isotactic polypropylene blends has been analyzed. The different samples were prepared by a two-stage process, that is, solvent casting followed by pressure molding. The analysis was carried out using techniques such as X-ray diffraction, differential scanning calorimetry (DSC), and thermomicroscopy. The experimental results show that both the components segregate a crystalline phase and that the overall crystallinity, as well as the crystallinity of each component, is affected by the sample composition. Some evidence of co-crystallization, at least for samples at low content in isotactic polypropylene, has been found. © 1994 John Wiley & Sons, Inc.

INTRODUCTION

In recent years the use of soluble Ziegler-Natta catalytic systems has provided new possibilities in stereospecific polymerization. Upon these, besides the polymerization of new systems like syndiotactic polystyrene,^{1,2} it is possible to control the stereoregularity between the two limits of high tactic and truly atactic systems. The homopolymerization of propylene, using, for instance, the Ewen's catalytic system,³ enables formation of high-molecular-weight stereoblock polypropylene. In these systems the absolute configuration of the tertiary carbon atom is maintained in isotactic blocks for a distance no longer than a few monomeric units (the number depends on the polymerization temperature), while the inversion of configuration is maintained in the following adjacent block. This chain microstructure causes a low degree of crystallinity⁴ and also interesting new properties like those typical of thermoplastic elastomers.⁵ The elastic behavior can be ascribed to the segregation of crystalline domains in an amorphous matrix, the crystalline domains having the role of physical crosslinks. In fact any elastic

behavior is lost at the melting temperature, which in these systems is observed at about 50°C. Polypropylene having elastomeric behavior can also be obtained using alumina-supported catalytic systems,⁶ and its elasticity is ascribed to a co-crystallization of the ether-soluble fraction with more stereoregular components to form a crosslinked physical network. Of course, a system based on the physical crosslinking can behave as an elastomer within the limits of thermal stability of the hard crystalline domains. In the pure stereoblock polypropylene the melting temperature is only a little above room temperature, and this dramatically reduces the possibilities of any practical use. On this basis, and in the assumption of co-crystallization, the blending with isotactic polypropylene can be a way to enlarge the range of temperature in which the elastic behavior is maintained. In the present study the thermal behavior of blends of stereoblock polypropylene with isotactic polypropylene has been investigated; the aim is to find evidence of co-crystallization phenomena, and in this case to find the conditions and the range of stability of the mixed crystalline domains.

^{*} To whom correspondence should be addressed.

[†] Permanent address: Materials Engineering Department, Universidade Federal de Sao Carlos, 13560 Sao Carlos (SP), Brazil.

Journal of Applied Polymer Science, Vol. 54, 2013–2021 (1994)
© 1994 John Wiley & Sons, Inc. CCC 0021-8995/94/132013-09

MATERIALS AND EXPERIMENTAL

The materials employed in this work were stereoblock polypropylene (sbiPP) previously used^{4,5} and

isotactic polypropylene (iPP) RAPRA. The blends were obtained by dissolving the two components in hot xylene and then casting a film at 80°C. The solvent casting was followed by compression molding at 190°C in a Carver hot press, and the molten films were rapidly quenched to 0°C in an ice-water bath.

Different samples were prepared in the whole composition range between the two pure components. Each sample is herein identified by the code sbiPP/iPP followed by a number indicating the weight content (percent) of iPP; i.e., sbiPP/iPP20 is a sample containing 80% in weight of sbiPP and 20% of iPP.

Wide-angle X-Ray diffraction (WAXS) patterns were obtained using a powder diffractometer (Philips PW1050). The radiation was the $\text{CuK}\alpha$ Ni filtered; the scan rate was 0.5°/min in the range 5–35° of 2θ .

The thermal behavior was analyzed by differential scanning calorimetry (DSC); the analysis was carried out using a Mettler TA 3000 DSC purged with nitrogen and chilled with liquid nitrogen. The thermal scanning was performed in the range of 60–200°C; the scanning rate was 10°/min on heating.

Thermomicroscopy was carried out using a Jenapol microscope equipped with a hot-stage THMS600 from Linkam. The intensity of the light transmitted through crossed polaroids was detected as a function of the temperature; the heating rate was 2°/min. The intensity (in arbitrary units) was measured by a Gossen Lunasix 3 exposimeter.

RESULTS

In Figure 1 we report the wide angle X-ray diffraction spectra of the sbiPP/iPP blends in the whole range of concentration, including the two pure components. The pure iPP shows the main peaks at 14.0, 16.8, 18.4, 21, 21.8, and 25.4 of 2θ , which are indicative of the α -form.⁷ The pure sbiPP shows a diffraction spectrum indicative of low crystallinity; the peak at 18.4 is not detectable and the intensity at 16.8 is higher than at 14. The first result is the consequence of the steric disorder. The last two facts seem to suggest the presence of the γ -form, as previously observed,⁵ even though in the present case the peak at 19.8 typical of γ -form,⁷ is not observed.

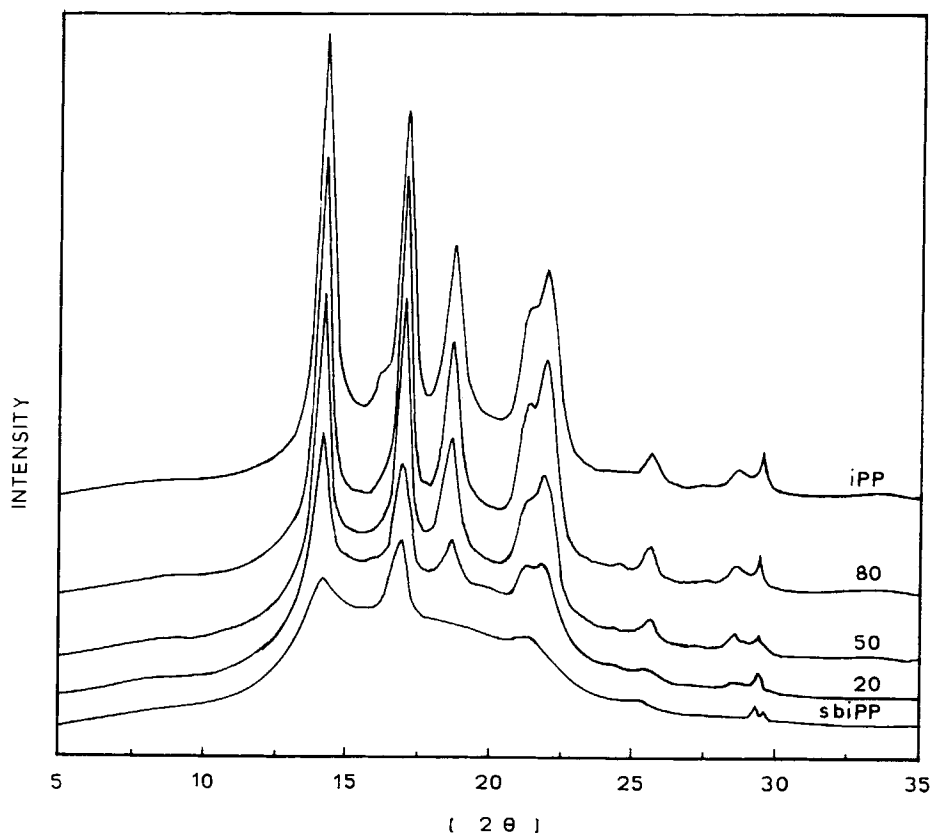


Figure 1 X-Ray diffraction spectra of the sbiPP/iPP blends with various iPP concentrations as shown.

Table I Crystallinity from X-ray Data

iPP%	X_c
0	16
20	26
50	36
80	47
100	50

As for the blends, the analysis was carried out on films obtained after the two-stage treatment, that is, casting from solvent followed by pressure molding. A progressive decrease of the crystallinity is observed going from the pure iPP to the pure sbiPP, while, on the basis both of the diffraction peaks and of the relative intensities, the crystalline phase seems to be the α -form, at least prevalently.

The crystallinity X_c was obtained from the area of the discrete diffraction peaks divided by the total diffraction area; the obtained results are reported in Table I.

The DSC thermograms, detected on the different samples, are reported in Figure 2. The pure sbiPP shows a glass transition at about -8°C and a wide

melting endotherm with a double peak having the relative maxima at 43 and 65°C , respectively. On the other hand, the pure iPP shows a single intense melting endotherm with the maximum centered at 164°C , as expected for isotactic polypropylene. The blends show two melting endotherms in the melting regions of each pure component, with intensities in first approximation depending on composition. The thermal data are reported in Table II, as melting temperature T_m , crystallinity $X_{c(1)}$ and $X_{c(2)}$, referred to each component (normalized to the actual content), and total crystallinity X_c , referred to the whole sample, all calculated using $\Delta H^\circ = 165 \text{ J/g}^8$ as thermodynamic melting enthalpy.

It is evident that the total crystallinity increases with increasing the iPP content, and the obtained values are in satisfactory agreement with the X-ray data. On the other hand, considering the $X_{c(1)}$ and $X_{c(2)}$ values, some more detailed information can be derived; the iPP crystallinity, normalized to the iPP content, fluctuates in a short range, 47–51%, except for sample sbiPP/iPP20 in which the calculated $X_{c(2)}$ is 43%. The crystallinity of the sbiPP decreases on increasing the iPP content, with a minimum in sample sbiPP/iPP50. In contrast to the pure component, in the melting region of sbiPP, a single peak

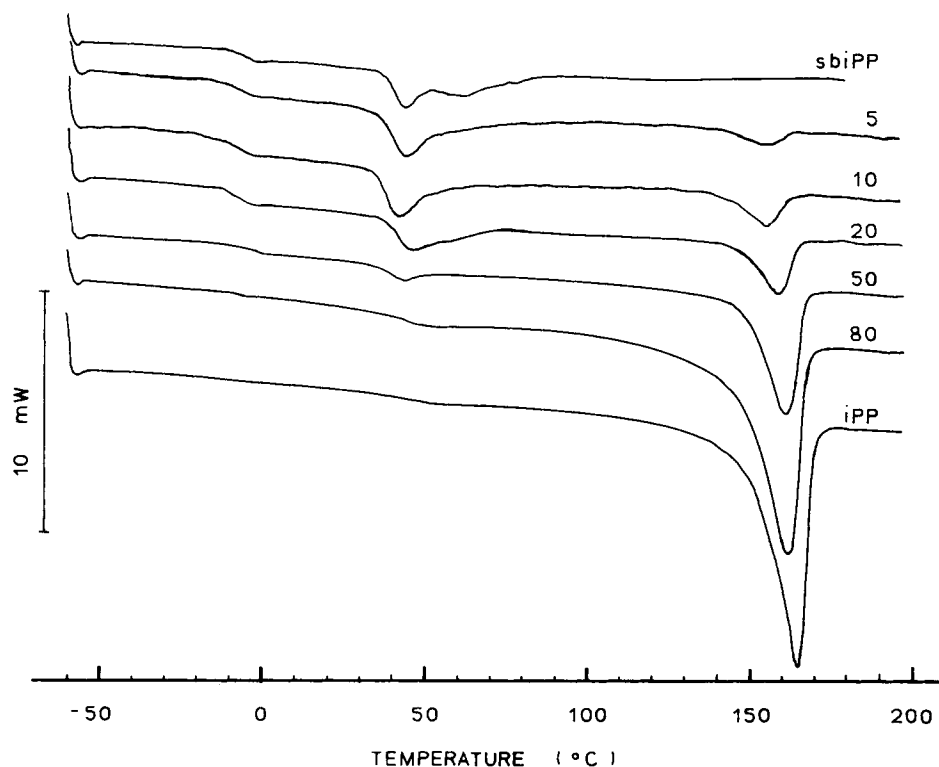


Figure 2 DSC thermograms of the sbiPP/iPP blends with various iPP concentrations. Scanning rate $10^\circ\text{C}/\text{min}$.

Table II Thermal Data

iPP (%)	sbiPP Phase		iPP Phase		
	T_m (°C)	$X_{c(1)}$ (%)	T_m (°C)	$X_{c(2)}$ (%)	X_c (%)
0	43.5 65.0	13	—	—	13
5	43.4	13	154.0	47	15
10	40.7	11	153.9	52	15
20	45.7	9	158.3	43	16
50	42.3	7	161.0	51	29
80	48.9	10	161.6	52	43
100	—	—	164.6	51	51

is observable, corresponding to a lower melting temperature. The peak is centered at a temperature that changes with the composition without any apparent trend. The melting temperature of the iPP phase increases on increasing the iPP content, but with a very evident step in the range of composition 10–20% of iPP.

The melting behavior of the different samples was also analyzed using thermal microscopy. A preliminary observation in cross-polarized light shows a radial orientation, consequent to the pressure molding followed by rapid quenching. The effect is a periodic change of the transmitted intensity on rotating the sample; therefore a direction corresponding

to the maximum in intensity can be selected, and in this direction the transmitted intensity was measured as a function of the temperature. The obtained results are reported in Figure 3. For the pure iPP, and for blends with high iPP content (including 50% of iPP), there is only one very detectable transition corresponding to the melting of the iPP crystalline phase. For sample sbiPP/iPP20 a continuous decrease of the intensity is observable in the whole temperature range, with a very evident accentuation in the range of melting of the two pure components. In sample sbiPP/iPP5 a transition in the range of melting of sbiPP is observable followed by a continuous decrease of intensity up to 150°C and, as ex-

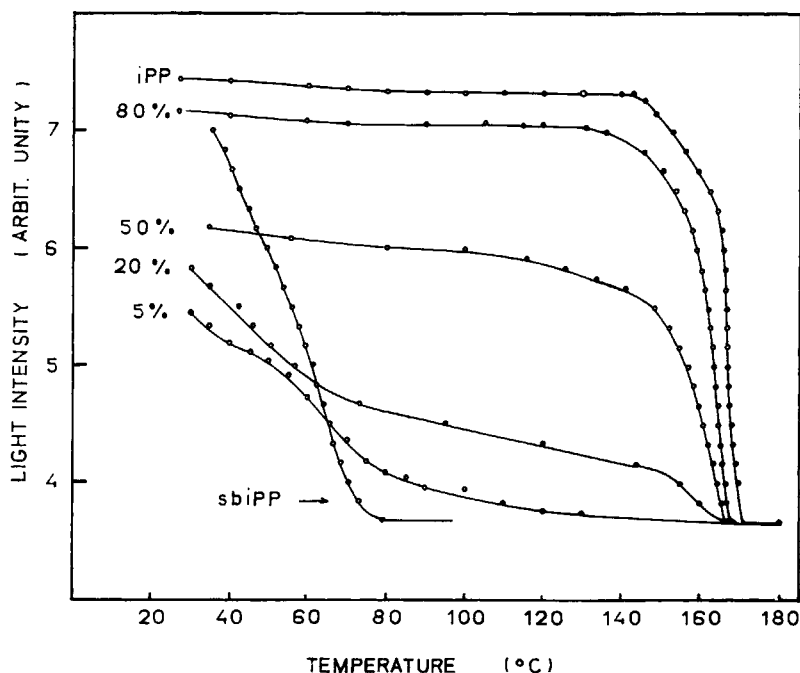


Figure 3 Transmitted light intensity (in arbitrary units) as a function of the temperature for the sbiPP/iPP blends with various iPP contents.

pected, for the pure sbiPP the intensity goes to the minimum at the end of its melting range, that is, at about 80°C.

In both techniques, DSC and thermomicroscopy, the analysis was also carried out during cooling. Figure 4 shows the crystallization temperature of the iPP phase as a function of its content in the blends. Two curves are shown; the first regards the nucleation temperature taken as the temperature at which the first birefringence domains appear in the microscope, using a cooling rate of 0.5°C/min. The second curve regards the temperature of maximum crystallization rate, taken as the temperature of the exotherm peak detected with the DSC at a cooling rate of 10°C/min. The nucleation temperature increases on increasing the iPP content going through a slight maximum for the blend sbiPP/iPP80. The effect is dramatically amplified when the temperature of maximum crystallization rate is considered. Also in this case the temperature goes through a maximum for the same composition, but drops about 8° going from this sample to the pure iPP.

The analysis of the thermal cycle, heating fol-

lowed by cooling, gives some further information, when carried out via thermomicroscopy. Figure 5 shows the transmitted light intensity detected on heating sample sbiPP/iPP5. The sample was aligned as reported above, and the intensity was recorded with the polarized light oriented at 0° and 45° (i.e., maximum and minimum transmitted light intensity, respectively). As shown, the maximum light intensity measured at 0° does not drop to zero above the melting of sbiPP (about 80°C) but rather reduces slowly, reaching the same intensity value measured at 45° (dark field) at about 140°C. At this temperature the sample shrinks slightly inducing a displacement of the analyzed area. Subsequent heating does not affect the measured light intensity (within the detection limits of the apparatus), but still some birefringent structure remains observable up to a critical temperature range of 150–160°C when it disappears completely with the melting of the iPP phase (154°C as measured by DSC).

The first heating run is not reproducible, and cooling to room temperature from any temperature, below this critical temperature range, intensities

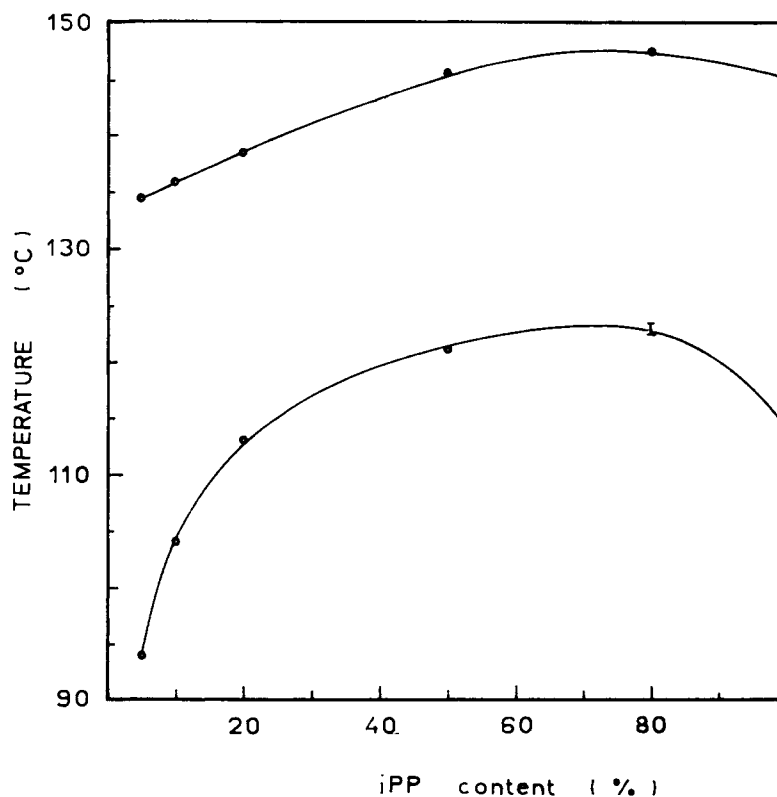


Figure 4 Recrystallization temperature of the iPP phase during cooling the sbiPP/iPP melt blends. Upper curve: nucleation temperature as measured by the thermomicroscope. Lower curve: temperature of maximum recrystallization rate as measured by the DSC exotherm.

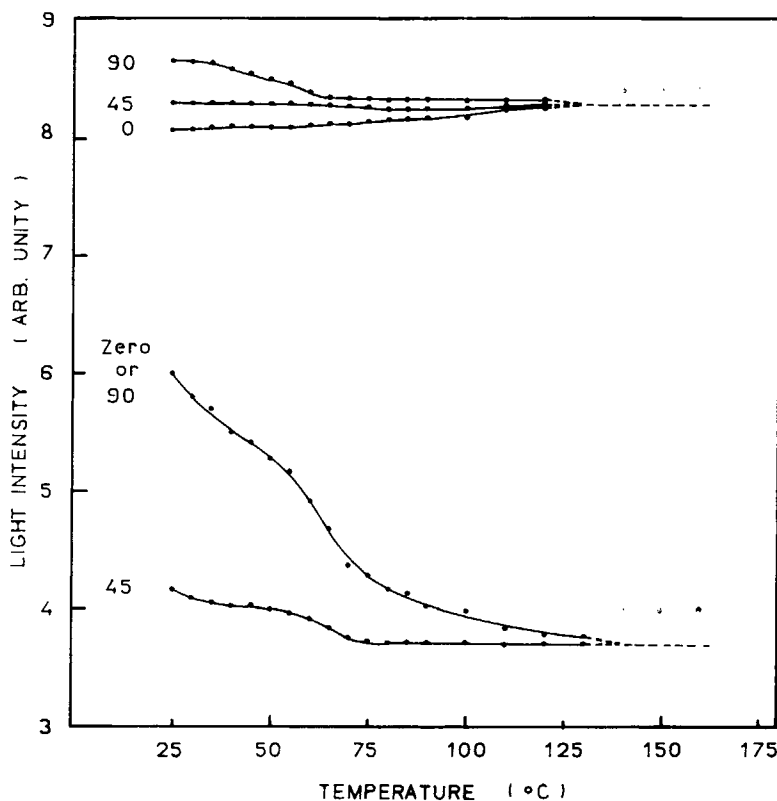


Figure 5 Transmitted intensity (in arbitrary units) as a function of the temperature for the sbiPP/iPP5 blend, measured at various directions (0° , -45° , and -90°) without (lower set of curves) and with (upper set) a λ filter.

much smaller than the initial values are observed. Moreover the intensity becomes independent on the sample orientation, and any periodicity with the polarization angle is strongly reduced. At room temperature the observed values slightly increase with time, but remain always lower than the initial ones. On heating again above 80°C the light intensity disappears, indicating that only the sbiPP phase has crystallized in a random orientation.

On the other hand if the sample is heated above the critical temperature range ($140\text{--}150^\circ\text{C}$) the birefringent structure will be destroyed and so during cooling the iPP phase recrystallizes at about 90°C showing an increase of the light intensity independent on the sample orientation. The crystallization is observable in the microscope as small but abundant needlelike segregated birefringent crystals. On cooling even further to the room temperature, the sbiPP phase also crystallizes. In any case the final intensity at room temperature is always lower than the starting value. If the analysis is carried out using a red filter (λ plate), the color pattern distribution on heating and on cooling confirms the irreversibility of the first run, with the loss of the radial orientation.

The first run can be reproduced only if the pressure molding treatment is once again carried out.

More complex is the trend of sample sbiPP/iPP10, and the influence of the thermal cycles on the physical behavior is in general so relevant that all the matter requires a specific attention; this will be considered in forthcoming studies.

DISCUSSION

The X-ray diffraction spectra indicate that the pure iPP crystallizes in α -form. The crystalline packing is predominantly the same in the different blends; at least there is not clear evidence suggesting a different conclusion. On the other hand, mainly on the basis of the relative intensities of the diffractions at 16.8° and 14° of 2θ , one can suggest that the pure sbiPP crystallizes in γ -form, as previously found.⁵ It is therefore reasonable to assume that the content of γ -form increases on increasing the content of sbiPP, even if there is not other experimental support.

The DSC data give more detailed information, and among these the first regards the number of the crystalline phases. It is clear that all the blends, as obtained by the two-stage process (solvent casting and pressure molding), show two melting endotherms indicating that for any composition each component is able to organize a crystalline phase. The crystallinity of the iPP component (normalized to its content) is very close to the value observed in the pure iPP, even for sample sbiPP/iPP5, where the content of iPP is very small. Sample sbiPP/iPP20 is an exception showing the minimum value of crystallinity (43%); this aspect will be considered more in detail later. It follows that the stereoblock does not affect in a significant way the crystallinity of the iPP, at least when the sample crystallizes during the rapid quenching that follows the pressure molding. A little different is the situation for the stereoblock component; in this case the crystallinity decreases, even if not dramatically, on increasing the iPP content, going through a minimum for the composition 1 : 1. The rate of crystallization of sbiPP is low when compared to the pure iPP,⁴ and for this reason probably the crystallization of the sbiPP component continues at room temperature after quenching, when the crystallization of iPP is concluded. This means that the crystallization of sbiPP occurs in a system in which the overall molecular mobility is reduced by the presence of a crystalline rigid component, and it is therefore reasonable to assume that the effect becomes more relevant on increasing the iPP content. In the same direction seems to point an other experimental evidence, i.e., the absence of the second melting peak observed at 65°C in the pure sbiPP. In fact the hindering effect due to the iPP is expected to be more relevant for the crystallization of thicker and ordered crystals, melting at higher temperature, being therefore only formed in the pure sbiPP.

Extending the attention to all the samples, some further indication can be deduced from the trend of the melting temperatures. It is evident that the melting of the iPP phase occurs at temperatures increasing as the iPP content increases; the same effect is observable for the melting temperature of the sbiPP component, again with the exclusion of the sample with the composition 1 : 1. It follows a capacity of the iPP component to improve the overall order degree, that on the other hand is deducible from the X_c values, both as given by the X-ray data and as deducible by the thermal data. This conclusion is apparently in contradiction with the previous observations regarding the crystallinity of each single component, which is substantially independent

on composition for the iPP phase, and weakly dependent on the composition for the sbiPP phase. However, the melting temperature is not affected by the crystallinity, but rather by the crystal thickness and quality, in terms of order degree.⁹ Therefore one can conclude on this aspect confirming once again the capacity of the iPP component to improve the order degree of the whole sample.

The optical analysis adds some decisive element to understand the phase organization of the analyzed samples; one can start from the data of Figure 3, which regards the first run detected on heating. At high iPP content only the melting of the iPP phase is very detectable; for samples sbiPP/iPP20 and sbiPP/iPP5 the transmitted intensity decreases in all the temperature range, indicating a melting process extended to all the range. In sample sbiPP/iPP20 the decrease of intensity between the melting of the two pure components is very appreciable; in this range a direct observation shows indeed the disappearance of birefringent elements in the optical field. This result suggests a wide distribution of the melting temperatures, indicative of a wide distribution of crystal thickness and order degree. Similarly the continuous decrease of intensity above the melting of the sbiPP phase in sample sbiPP/iPP5 can be assumed as indicative of the same wide distribution of melting temperatures. The question is now the following: Can this experimental result be assumed as an evidence of co-crystallization phenomena?

Most probably the answer is yes, not only from the data already shown but also on the basis of some complementary observation. The total crystallinity X_c (calculated via thermal data) is underestimated if compared with X_c (calculated via X-ray diffraction), particularly for the intermediate compositions. Sample sbiPP/iPP20 shows the minimum value for $X_{c(2)}$ and also the wider disagreement between the two techniques. While the crystallinity obtained via X-ray diffraction includes any diffracting volume element, the crystallinity calculated via thermal data is based on the separate integration of the two melting endotherms relative to each component. In both cases the definition of the baseline (the diffuse scattering of the amorphous component in the case of X-ray) contains some approximation. In the case of sample sbiPP/iPP20, for which the wider disagreement is observed, we attempted an integration of the thermogram over all the temperature range in which the optical analysis indicates the continuous decrease in transmitted intensity. The thermograms are shown in Figure 6 for three different scanning rates, and the calculated crystallin-

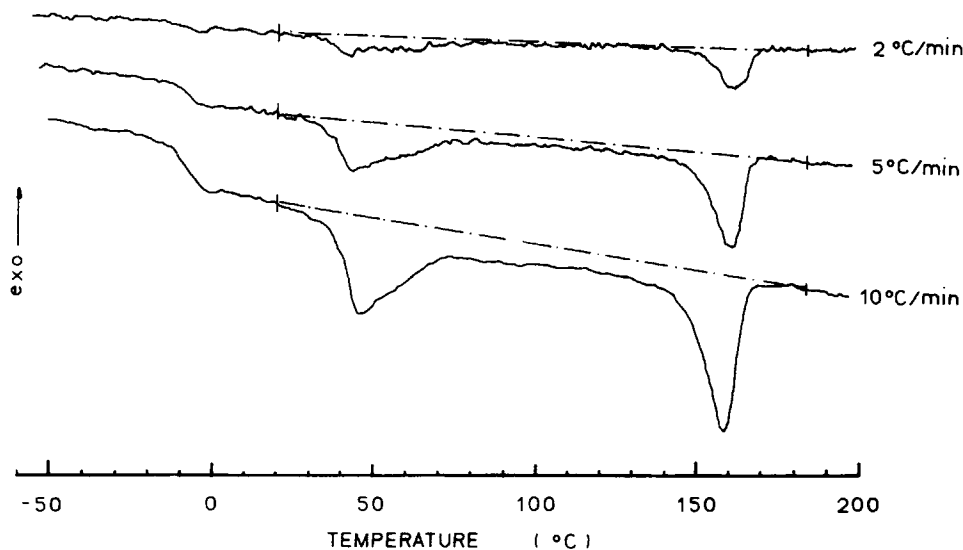


Figure 6 DSC thermograms of sbiPP/iPP20 blend at different scanning rates. The melting enthalpy was obtained by integration over all the melting range.

ity are reported in Table III, using the same codes adopted in Table II.

The overall crystallinity X_c , here obtained by integration over all the melting range, now compares with the X-ray data. The progressive increase of X_c , $X_{c(2)}$ [weak being the effect on $X_{c(1)}$] and $T_{m(2)}$ on decreasing the scanning rate, all are indicative of melting and re-crystallization phenomena during the scanning; this is typical of nonequilibrium phenomena that are, in general, present in systems rapidly crystallized by quenching, but in the present case widely expected for crystals formed by co-crystallization of high tactic and low tactic sequences. On the basis of this complementary experiment on sample sbiPP/iPP20 it seems extremely reasonable to assume the presence of co-crystallization phenomena, at least for samples at low iPP content. It is here interesting to point out that co-crystallization is not observable in isotactic polypropylene/atactic polypropylene blends.¹⁰ This means that the co-crystallization requires steric order even if low and extended to short sequences only.

Table III Crystallinity of Sample sbiPP/iPP20

Rate (°C/min)	$X_{c(1)}$	$X_{c(2)}$	X_c	$T_{m(2)}$
10	9	43	25	157
5	13	47	27	161
2	13	64	29	162

As far as it concerns the crystallization data of Figure 4, regarding the nucleation temperature and the maximum crystallization rate of the crystalline iPP phase, it seems that the melting temperature of iPP, which decreases as the iPP content decreases, reflects on the crystallization parameters; in fact different samples, at the same temperature in the crystallization range, are indeed in different supercooling conditions. However, this could explain the observed results with the exclusion of the pure iPP, which is comparable with the sample sbiPP/iPP50 for the nucleation temperature and with the sample sbiPP/iPP20 for the crystallization rate. Therefore the different supercooling cannot be the only explanation, and an additive effect must be suggested. A mechanism could be related to the auto-hindering that the just formed crystals of iPP plays on the further crystalline growing; this effect is reduced by the presence of sbiPP, fluid at the temperature of crystallization of iPP, and therefore acting as diluent on the system. This effect can indeed reflect on the crystallization rate in the observed direction.

The last aspect to consider regards the irreversibility phenomena observed when thermal cycles are carried out. The first effect regards the relaxation of the radial orientation on heating, and the second regards some irreversible mechanism observable in the crystallization of the iPP component in samples at low iPP content. These aspects, which are very complex and give the key to understand the mechanical behavior of the different blends,¹¹ will be specifically considered in forthcoming studies.

The authors sincerely thank Dr. C. Pellecchia (Dip. di Fisica, Università di Salerno) for the synthesis of stereoblock polypropylene and for many useful discussions.

One of us (S. C.) sincerely acknowledges the financial support given by FAPESP (Research Founding Institution, Brazil).

REFERENCES

1. N. Ishihara, T. Seimiya, M. Kuramoto, and M. Uoi, *Macromolecules*, **19**, 2465 (1986).
2. C. Pellecchia, P. Longo, A. Grassi, P. Ammendola, and A. Zambelli, *Makromol. Chem. Rapid Commun.*, **8**, 277 (1987).
3. J. A. Ewen, *J. Am. Chem. Soc.*, **106**, 6355 (1984).
4. F. de Candia and R. Russo, *Thermochim. Acta*, **177**, 221 (1991).
5. F. de Candia, R. Russo, and V. Vittoria, *Makromol. Chem.*, **189**, 815 (1988).
6. J. W. Colette, C. W. Tullock, R. N. MacDonald, W. H. Buck, A. C. L. Su, J. R. Harrell, R. Mulhaupt, and B. C. Anderson, *Macromolecules*, **22**, 3851 (1989).
7. A. Turner Jones, J. M. Aizlewood, and D. R. Beckett, *Makromol. Chem.*, **75**, 134 (1964).
8. J. Grebowich, J. F. Lau, and B. Wunderlich, *J. Polym. Sci. Polym. Symp.*, **71**, 19 (1984).
9. See, e.g., D. C. Bassett, *Principle of Polymer Morphology*, Cambridge University Press, Cambridge, 1981.
10. D. J. Lohse and G. P. Wissler, *J. Mat. Sci.*, **26**, 743 (1991).
11. S. Canevarolo, F. de Candia, R. Russo, to appear.

Received January 24, 1994

Accepted May 10, 1994